MicroRNA-34a-3p inhibits proliferation of rheumatoid arthritis fibroblast-like synoviocytes

CHUNFENG HOU[1,2*], DAN WANG[1,2*] and LIHUA ZHANG[1,2]

[1]Department of Rheumatology, Jining No. 1 People's Hospital, Jining, Shandong 272011;
[2]Department of Rheumatology, Affiliated Jining No. 1 People's Hospital of Jining Medical University, Jining Medical University, Jining, Shandong 272067, P.R. China

Received September 4, 2018; Accepted April 10, 2019

DOI: 10.3892/mmr.2019.10516

Abstract. Rheumatoid arthritis (RA) is a chronic inflammatory joint disease characterized by synovial inflammation. Fibroblast-like synoviocytes (FLS) serve a vital role in the initiation and perpetuation of the immune response in patients with RA. The present study aimed to investigate the potential role of microRNA (miR)-34a-3p in the pathogenesis of RA. FLS were collected from patients with RA and osteoarthritis (OA). The miR-34a-3p mimics and inhibitor vectors were constructed and transfected into RAFLS using Lipofectamine® 2000. Cell proliferation was determined by Cell Counting kit-8 assay and cell cycle progression was analyzed by flow cytometry. In addition, the expression levels of cell cycle control genes, matrix metalloproteinase (MMP)-1 and MMP-9, and pro-inflammatory cytokines were detected by reverse transcription-quantitative polymerase chain reaction and western blot analysis. The potential targets of miR-34a-3p were predicted by TargetScan and MiRWalk; the target genes were further verified using a luciferase reporter assay. The expression levels of miR-34a-3p were generally lower in RAFLS compared with in OAFLS. miR-34a-3p overexpression significantly inhibited the proliferation of FLS ($P<0.01$) by suppressing the expression levels of cyclin-dependent kinase 2, cell division cycle 25A and cyclin D1 ($P<0.01$), and arresting FLS cell cycle progression at the G_1 phase. Furthermore, the expression levels of MMP-1 and 9 were markedly decreased, as were the mRNA and protein expression levels of pro-inflammatory cytokines (tumor necrosis factor α and interleukin 6; $P<0.01$). Murine double minute 4 (MDM4) was predicted and verified as a potential target gene of miR-34a-3p; the 547-554 nt position of the MDM4 3'-untranslated region harbored one potential binding site for miR-204-3p. The results of the present study indicated that miR-34a-3p may be considered a promising therapeutic target for RA through inhibiting FLS proliferation and suppressing the production of pro-inflammatory cytokines and MMPs.

Correspondence to: Dr Lihua Zhang, Department of Rheumatology, Jining No. 1 People's Hospital, 6 Jiankang Road, Jining, Shandong 272011, P.R. China
E-mail: zhanglihua_lhzh@163.com

*Contributed equally

Key words: synovial fibroblast, articular cartilage, synovium, pro-inflammatory cytokines, matrix metalloproteinases

Introduction

Rheumatoid arthritis (RA) is a common chronic inflammatory joint disease characterized by synovitis, synovial hyperplasia, pannus formation, and the destruction of bone and cartilage (1). In China, the incidence of RA is ~0.3% (2), which is 0.7% lower compared with the world average level; however, it has a high disability rate (3). Although the causes of RA remain to be elucidated, a previous study suggested that fibroblast-like synoviocytes (FLS), also known as synovial fibroblasts, exert a crucial effect on initiation and perpetuation of the immune response in patients with RA (4). FLS and macrophages are two cell types composing the lining of normal synovial tissue. In the event of RA, abnormal activation of macrophages can promote FLS to produce pro-inflammatory cytokines and matrix metalloproteinase (MMPs). These pro-inflammatory cytokines are capable of recruiting more inflammatory cells and support continued arthropathy (5). In addition, MMPs have the ability to degrade the extracellular matrix (ECM) resulting in damage to cartilage and bone; for example, MMP-1 can effectively break down collagen type II, which is the basis of articular cartilage (6). Furthermore, tumor necrosis factor (TNF)-α and interleukin (IL)-1, secreted in response to lipopolysaccharide, can directly or indirectly induce the proliferation of osteoclasts by inducing nuclear factor-κB ligand to bind to the corresponding receptor (7,8). Consequently, the activation of osteoclasts may lead to bone erosion and inflammatory arthritis (9). Although a number of effective and hypotoxic medicines have been developed, the long treatment cycle of RA notably increases the incidence of adverse reactions. Therefore, it is essential to understand the molecular mechanism underlying RA and provide evidence for personalized medicine.

MicroRNAs (miRNAs/miRs) are 18-25 nt long, endogenous non-coding RNAs, which modulate the expression of one or more genes by regulating the degradation or translational repression of mRNA. The molecular mechanisms underlying

the synthesis and function of miRNAs have been widely studied (10). As molecular biology has advanced, more studies have provided evidence for a vital role of miRNAs in the pathogenesis of RA (11,12). In 2011, 13 differentially expressed miRNAs were identified by comparing the differential expression of miRNAs in rheumatoid synovial fluid monocytes with normal peripheral blood monocytes using a miRNA microarray; miR-34a-5p was one of these differentially expressed miRNAs (13). Previous studies have reported that miR-34a-5p is involved in the development of RA (14,15); however, the underlying mechanism of miR-34a-3p on FLS remains to be elucidated. The present study constructed miR-34a-3p mimics and inhibitor vectors to further investigate its role in RA.

Materials and methods

Patient samples and cell culture. Synovial tissue specimens of RA (7 males and 13 females; average age, 52 years old) and osteoarthritis (OA, 8 males and 12 females; average age, 48 years old) were obtained from patients during total knee replacement surgery or arthroscopy at the Jining No. 1 People's Hospital from January 2016 to February 2017. In addition, arthroscopic biopsies from healthy individuals who underwent arthroscopic surgery for knee meniscus injuries or cruciate ligament rupture and had no history of autoimmune diseases were recruited as a control group (11 males and 9 females; average age, 42 years old). Written informed consent was obtained from all patients in this study, and the study was approved by the Medical Ethical Review Committee of Jining No. 1 People's Hospital. All RA and OA patients fulfilled the American College of Rheumatology criteria for the classification of the disease (16). FLS were obtained from patients with RA and OA (RAFLS and OAFLS) by incubating synovial tissue samples with Dulbecco's modified Eagle's medium (DMEM; cat. no. D5030; Sigma-Aldrich; Merck KGaA) containing type II collagenase (1 mg/ml; Sigma-Aldrich; Merck KGaA) in a humidified incubator containing 5% CO_2 at 37˚C for 6 h. The same volume of 0.25% trypsin was then added to the culture medium. Following filtration through a 70-μm cell strainer, FLS were cultured in complete medium supplemented with 10% fetal bovine serum (FBS; Gibco; Thermo Fisher Scientific, Inc.), 100 IU/ml penicillin and 10 μg/ml streptomycin in a humidified incubator containing 5% CO_2 at 37˚C.

Cell transfection. The sequence of miR-34a-3p was obtained from miRbase (MIMAT0004557, http://www.mirbase.org/textsearch.shtml?q=miR-34a-3p). FLS were seeded into 12-well plates ($1x10^5$ cells/well) and transfection was conducted using Lipofectamine® 2000 (Invitrogen; Thermo Fisher Scientific, Inc.). Briefly, when cell confluence reached 50%, miR-34a-3p mimics (5'-CAAUCAGCAAGUAUACUGCCU-3'), miR-34a-3p inhibitor (5'-ACAACCAGCUAAGACACUGCCA-3') and non-sense single-strand RNA (5'-CAGUACUUUUGUGUAGUACAA-3'; Invitrogen; Thermo Fisher Scientific, Inc.) were diluted in DMEM (50 ng/ml), and were added to the cells alongside 5 μl Lipofectamine® 2000. The mixture was incubated at 37˚C in a humidified atmosphere containing 5% CO_2 for 6 h, after which the medium was replaced with complete medium. The transfection efficiencies of miR-34a-3p mimics and inhibitor vectors were assessed after 24 h.

Cell proliferation assay. The non-transfected or transfected FLS were cultured in 96-well plates ($3x10^5$ cells/well) under 5% CO_2 and 37˚C. Cells were harvested at 0, 24 and 48 h, respectively. Subsequently, 10% Cell Counting kit (CCK)-8 reagent (Dojindo Molecular Technologies, Inc.) was added to the cell culture medium and the plates were maintained at room temperature for 4 h. The absorbance was then measured at 450 nm using a microplate reader (Thermo Fisher Scientific, Inc.).

Flow cytometry. Cell cycle analysis was carried out as previously described using propidium iodide (PI) staining (17). FLS transfected with miR-34a-3p mimics, inhibitor or negative control (NC) vectors were seeded in 6-well plates ($1x10^6$ cells), and incubated for 24 h until cell confluence reached 100%. Cells in each group were harvested and washed with cold PBS, after which they were fixed with 70% cold ethanol at 4˚C overnight. Cells were then washed and resuspended in PBS, and were incubated in buffer containing 50 μg/ml PI and 10 μg/ml RNase A (Beyotime Institute of Biotechnology) for 30 min in the dark at 37˚C. The fraction of cells in the G_1, S, and G_2 phases of the cell cycle was analyzed using a Coulter Epics XL flow cytometer (BD Biosciences). The data were acquired and analyzed using FACSDiva software (version 4.1; BD Biosciences). Integration of the area under the curve for each of the cell cycle phases was performed with ModFit LT software (version 3.3; BD Biosciences).

Reverse transcription-quantitative polymerase chain reaction (RT-qPCR). For detection of miRNA expression levels, miRNAs were isolated from FLS using a miRNeasy Mini kit (Qiagen GmbH), and purified by TURBO DNA-free kit (Invitrogen; Thermo Fisher Scientific, Inc.). Subsequently, RNA was reverse transcribed to cDNA using a miScript II RT kit (Qiagen GmbH) as previously described (18); the samples were incubated at 37˚C for 60 min, 95˚C for 5 min and were then maintained at 4˚C. The relative expression levels of miRNAs were analyzed using the miScript SYBR Green PCR kit (Qiagen GmbH). Each qPCR was performed in a final volume of 20 μl containing 1X QuantiTect SYBR Green PCR Master mix (Qiagen GmbH), 2 μl cDNA and 0.5 mM each primer. The miScript Universal primer was used as the reverse primer for miRNA detection. In addition, for detection of mRNA expression levels, total RNA was extracted with TRIzol® reagent (Invitrogen; Thermo Fisher Scientific, Inc.) and reverse transcribed to cDNA using the Prime Script RT reagent kit (Takara Bio, Inc.). The RT reaction conditions were as follows: 65˚C for 5 min, 30˚C for 6 min and 50˚C for 60 min. qPCR was performed using the SYBR green detection kit (Takara Bio, Inc.). The miRNA and mRNA levels were analyzed using an ABI 7500 real-time PCR system (Applied Biosystems; Thermo Fisher Scientific, Inc.). For detection of mRNA, the 20 μl reaction system consisted of 10 μl 2X SYBR green master mix, 7 μl H_2O, 2 μl primers (10 μM) and 1 μl template DNA. The reaction mixtures were denatured at 95˚C for 15 min, followed by 40 cycles of annealing at 94˚C for 15 sec, 55˚C for 30 sec and 70˚C for 30 sec. U6 was employed as the internal reference for miRNA and β-actin was the internal reference for mRNA. All samples were analyzed in triplicate, and the relative expression levels were quantified using the $2^{-\Delta\Delta Cq}$ method (19). All primers are listed in Table I.

Table I. Primers for reverse transcription-quantitative PCR.

Gene name	Primer sequences
CDK2	Forward: 5'-CAGTACTGCCATCCGAGAGA-3'
	Reverse: 5'-GAATGCCAGTGAGAGCAGAG-3'
CDC25A	Forward: 5'-CCTCCGAGTCAACAGATTCA-3'
	Reverse: 5'-GGGTCGATGAGCTGAAAGAT-3'
Cyclin D1	Forward: 5'-GTCTTCCCGCTGGCCATGAAC TAC-3'
	Reverse: 5'-GGAAGCGTGTGAGGCGGTAGT AGG-3
MMP-1	Forward: 5'-AAATGCAGGAATTCTTTGGG-3'
	Reverse: 5'-ATGGTCCACATCTGCTCTTG-3
MMP-9	Forward: 5'-TTGACAGCGACAAGAAGTGG-3'
	Reverse: 5'-GGCACAGTAGTGGCCGTAG-3
TNF-α	Forward: 5'-CATCTTCTCAAAATTCGAGTG ACAA-3'
	Reverse: 5'-TGGGAGTAGACAAGGTACAA CCC-3'
IL-6	Forward: 5'-AGTTGCCTTCTTGGGACTGA-3'
	Reverse: 5'-TCCACGATTTCCCAGAGAAC-3
MDM4	Forward: 5'-AGGTGCGCAAGGTGAAATGT-3'
	Reverse: 5'-CCATATGCTGCTCCTG CTGAT-3'
TRAF3	Forward: 5'-ACTGCAAGAGTCAGGTTCCG-3'
	Reverse: 5'-CAAGTGTGCACTCAACTCGC-3
TRAF1	Forward: 5'-CATGCAGGAGCATGAGGCT ACC-3'
	Reverse: 5'-CCACCACCCTCTGCTCCAAGC-3
PTPN11	Forward: 5'-TCAGCACAGAAATAGATGTG-3'
	Reverse: 5'-TGCTTATCAAAAGGTAGTCA-3'
XIAP	Forward: 5'-GTGGTGGAAAACTGAAAAAT TGG-3'
	Reverse: 5'-GAAAGTGTCGCCTGTGTTC TGA-3
β-actin	Forward: 5'-CCTGGCACCCAGCACAAT-3'
	Reverse: 5'-GGGCCGGACTCGTCATAC-3
U6	Forward: 5'-CTCGCTTCGGCAGCACATA-3'
	Reverse: 5'-AACGATTCACGAATTTGCGTC-3

CDK2, cyclin-dependent kinase 2; CDC25A, cell division cycle 25A; IL-6, interleukin 6; MDM4, murine double minute 4; MMP, matrix metalloproteinase; PTPN11, protein tyrosine phosphatase non-receptor type 11; TNF-α, tumor necrosis factor α; TRAF, TNF receptor-associated factor; XIAP, X-linked inhibitor of apoptosis.

Western blot analysis. Total protein of tissues and cells were lysed in 150 μl RIPA lysis buffer containing 1% phenylmethanesulfonyl fluoride (PMSF; Beyotime Institute of Biotechnology) according to the manufacturer's instructions. Protein concentration was quantified using a bicinchoninic acid protein assay (Takara Bio, Inc.), and 50 μg proteins were separated by 10% SDS-PAGE prior to being transferred onto a polyvinylidene difluoride (PVDF) membrane (EMD Millipore). The PVDF membrane was blocked with 5% nonfat milk in in PBS containing 0.1% Tween-20 for 1 h at room temperature and was then incubated with primary antibodies at 4˚C overnight. The primary antibodies were as follow: Anti-cyclin-dependent kinase 2 (CDK2; cat. no. 2546), anti-cell division cycle 25A (CDC25A; cat. no. 3652), anti-cyclin D1 (cat. no. 2978), anti-MMP-9 (cat. no. 2270), anti-tumor necrosis factor (TNF)-α (cat. no. 3707) and anti-interleukin (IL)-6 (cat. no. 12153; all from Cell Signaling Technology, Inc.), β-actin (cat. no. ab8226; Abcam) and anti-MMP-1 (cat. no. ab137332; Abcam). All primary antibodies were used at a dilution of 1:1,000. Subsequently, the membrane was incubated with goat anti-rabbit immunoglobulin G horseradish peroxidase-linked secondary antibodies (1:2,000; cat. no. 7074, Cell Signaling Technology, Inc.) for 1 h at room temperature. Blots were visualized using an enhanced chemiluminescence reagent (cat. no. 32106; Thermo Fisher Scientific, Inc.). Semi-quantification of image density was performed using ImageJ version 1.38 software (National Institutes of Health).

miR-34a-3p target prediction and luciferase reporter assay. The potential targets of miR-34a-3p were predicted using TargetScan (www.targetscan.org/vert_72) and MiRWalk 2.0 (mirwalk.umm.uni-heidelberg.de). Subsequently, the predicted target genes were investigated using a luciferase reporter assay. Briefly, miR-34a-3p was inserted into a GV272 vector (Shanghai GeneChem Co., Ltd.) and fragments containing a miR-34a-3p-binding site in the 3'-untranslated region (UTR) of predicted genes were cloned into a GV268 plasmid vector (Shanghai GeneChem Co., Ltd.). The QuikChange II Site-Directed Mutagenesis kit (Agilent Technologies, Inc.) was used to mutate the binding sites; the mutated fragments were also inserted into a GV268 plasmid vector (3'-UTR mut).

Luciferase reporter assay was performed on the 293 cell line (cat. no. CRL-3216; ATCC) using a Dual-Luciferase® Reporter Assay system (cat. no. E1910; Promega Corporation). Briefly, 293 cells at a density of $4x10^4$ were transfected with 50 ng GV272-miR-204-3p, and 40 nM of either control GV268-3'-UTR or GV268-3'-UTR mut by Lipofectamine® 2000. After 48 h, 293 cells were lysed with 200 μl 1% sodium dodecyl sulfate (SDS) and separated by centrifugation at 15,000 x g for 3 min at 4˚C. The prepared dual luciferase reporter mixture was added to the supernatant of lysed cells and the relative luciferase activity normalized against *Renilla* luciferase was immediately measured using a Synergy™ 2 luminometer (BioTek Instruments, Inc.).

Statistical analysis. Statistical analysis was detected using GraphPad Prism version 6.0 software (GraphPad Software, Inc.). All data are presented as the means ± standard deviation. Differences were analyzed using one-way analysis of variance followed by Tukey's multiple comparison test. $P<0.05$ was considered to indicate a statistically significant difference.

Results

miR-34a-3p expression is decreased in FLS from patients with RA. To identify the potential effect of miR-34a-3p on RA, the expression levels of miR-34a-3p were compared between different groups. The FLS purified from patients with RA

and OA were incubated under the same conditions and the results of RT-qPCR demonstrated that the expression levels of miR-34a-3p were generally lower in RAFLS compared with in OAFLS and normal FLS (Fig. 1). This result indicated the potential function of miR-34a-3p in the pathogenesis of RA.

Increased expression levels of miR-34a-3p inhibit the proliferation and cell cycle progression of RAFLS. To investigate the potential effects of miR-34a-3p on RAFLS, miR-34a-3p mimics and inhibitor vectors were transfected into RAFLS (Fig. 2A). As demonstrated in Fig. 2B, upregulated miR-34a-3p expression had an inhibitory effect on FLS proliferation (P<0.01). Therefore, the effects of miR-34a-3p on the cell cycle of FLS were further investigated. The results of flow cytometry were consistent with the CCK-8 assay; the number of miR-34a-3p mimics-transfected FLS in G_1 phase was significantly higher compared with in the control group (P<0.01), which suggested that high miR-34a-3p expression may effectively inhibit the cell cycle of FLS (Fig. 2C and D). By contrast, knockdown of miR-34a-3p promoted the cell cycle; however, this was not significant.

High miR-34-3p expression suppresses the expression levels of cell cycle control genes. The cell cycle control genes serve a crucial role in progression of the cell cycle. To further verify the inhibitory effects of miR-34a-3p on the cell cycle of RAFLS, the expression levels of several cell cycle control genes (CDK2, CDC25A and cyclin D1) were measured. As demonstrated in Fig. 3A-C, the transcriptional and post-transcriptional levels of these genes were significantly decreased, compared with in the control and NC groups (P<0.01). The inhibitory effects of miR-34a-3p were most marked on the mRNA and protein expression levels of CDK2. Conversely, the miR-34a-3p inhibitor vector appeared to exert little effects on the cell cycle control genes. These results further verified that miR-34a-3p had an inhibitory effect on the cell cycle progression of RAFLS.

Increased miR-34a-3p expression inhibits MMPs and pro-inflammatory cytokines in RAFLS. It has been reported that RAFLS can promote the expression levels of MMPs and pro-inflammatory cytokines, thus resulting in the destruction of synovial tissue (20). The present study examined the mRNA and protein expression levels of two MMPs (MMP-1 and MMP-9) and two pro-inflammatory cytokines (Fig. 4A-C). It was observed that the expression levels of MMP-1 and MMP-9 were significantly decreased in the miR-34a-3p mimics group compared with in the control group (P<0.01), which suggested that miR-34a-3p may protect the articular cartilage through inhibiting the expression levels of MMPs. In addition, miR-34a-3p significantly suppressed the expression levels of TNF-α and IL-6 (P<0.01); this may result in resistance to inflammation-induced bone destruction. Conversely, inhibition of miR-34a-3p promoted the production of MMPs and pro-inflammatory cytokines, but not significantly.

Affinity of miR-34a-3p to murine double minute 4 (MDM4) is greater compared with TNF receptor-associated factor (TRAF) 3. Two prediction algorithms (TargetScan and mirWalk) were combined to identify the potential target genes of miR-34a-3p;

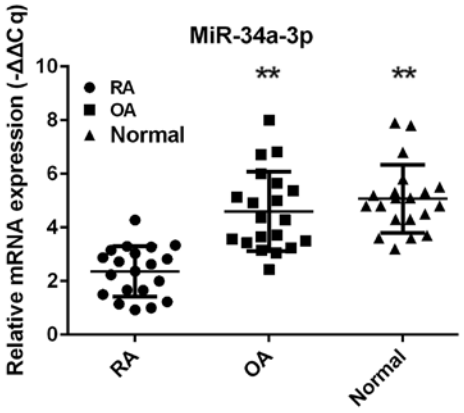

Figure 1. Expression levels of miR-34a-3p in RAFLS are generally lower compared with in OAFLS. Synovial tissue specimens from patients with RA (n=20) and OA (OA, n=20) who underwent total knee replacement surgery, and healthy individuals (n=20) who underwent synovial biopsies, and FLS were cultured under the same conditions. The expression levels of miR-34a-3p were measured by reverse transcription-quantitative polymerase chain reaction. β-actin was detected as an internal control. Each value represents the mean ± standard deviation. **P<0.01 vs. RA group. FLS, fibroblast-like synoviocytes; miR, microRNA; OA, osteoarthritis; RA, rheumatoid arthritis.

five predicted target genes were identified, MDM4, TRAF3, TRAF1, protein tyrosine phosphatase non-receptor type 11 and X-linked inhibitor of apoptosis (XIAP). As determined by RT-qPCR analysis, the expression levels of four genes (MDM4, TRAF3, TRAF1 and XIAP) were significantly decreased in the miR-34a-3p mimics group (P<0.01), and the inhibitory effects of miR-34a-3p mimics were the most marked on MDM4 and TRAF3 (Fig 5A). As shown in Fig. 5B, the 547-554 nt position of the MDM4 3'-UTR harbored one potential binding site for miR-204-3p (seven bases), whereas the 5700-5706 nt position of the TRAF3 3'-UTR included a potential binding site for miR-204-3p (six bases). MDM4 and TRAF3 were therefore considered potential target genes of miR-34a-3p.

Dual luciferase reporter plasmids were constructed to further identify the association between miR-34a-3p and MDM4 or TRAF3. The luciferase activity in the miR-34a-3p + MDM4 3'-UTR group was significantly reduced compared with in the Con + MDM4 3'-UTR group (P<0.01). The luciferase activity in the miR-34a-3p + MDM4 3'-UTR mut group exhibited no difference compared with in the control group. miR-34a-3p also had an effective inhibitory effect on the luciferase activity of TRAF3 3'-UTR (P<0.01), whereas the luciferase activity of the miR-34a-3p + TRAF 3'-UTR mut group exhibited no difference compared with in the Con + TRAF3 3'-UTR group. Notably, the inhibitory effects of miR-34a-3p on MDM4 luciferase activity were more marked compared with on TRAF3 luciferase activity (Fig. 5C). These findings suggested that miR-34a-3p possessed a stronger affinity to MDM4 compared with to TRAF3.

Discussion

The present study aimed to determine the function of the miR-34 family, which has been reported to serve an important role in the progression of apoptotic cell death (21,22). It has been observed that miR-34a-3p has functions opposite to other miR-34 family members, including miR-34a-5p,

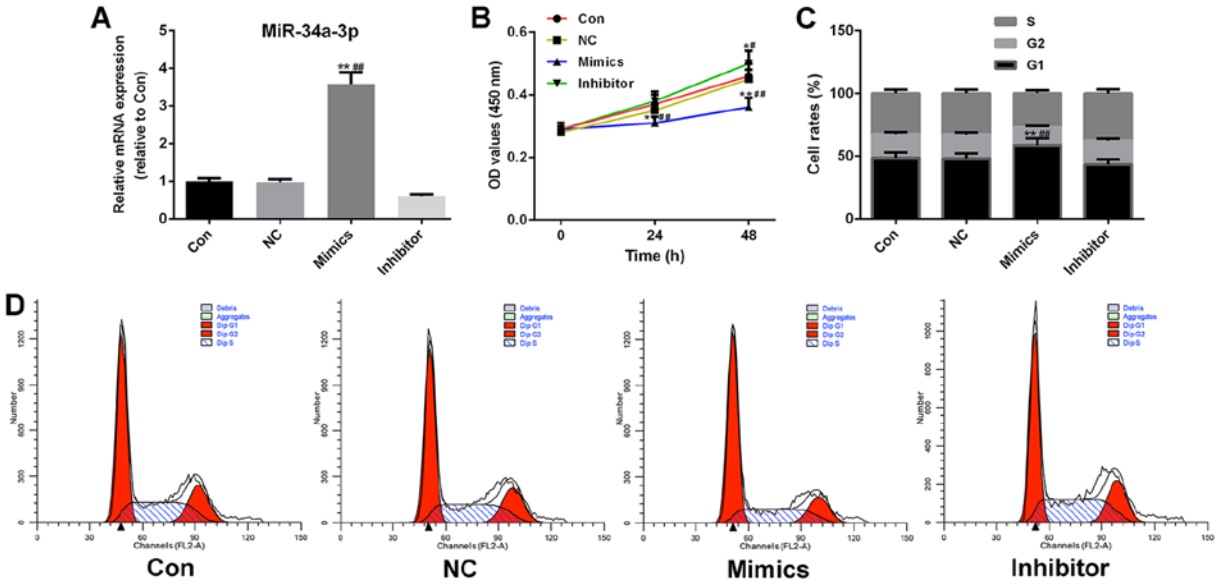

Figure 2. Increased miR-34a-3p expression inhibits the proliferation and cell cycle progression of RAFLS. miR-34a-3p mimics and inhibitor vectors were constructed and transfected into RAFLS. (A) Transfection efficiencies of all vectors were assessed by reverse transcription-quantitative polymerase chain reaction. β-actin was detected as an internal control. (B) Cell Counting kit-8 assay was performed to determine the proliferation of FLS at 0, 24 and 48 h. (C and D) Cell cycle analysis was conducted using propidium iodide staining and flow cytometry. Each value represents the mean ± standard deviation (n=3). *P<0.05, **P<0.01 vs. Con group; $^{\#}$P<0.05, $^{\#\#}$P<0.01 vs. NC group. Con, control; FLS, fibroblast-like synoviocytes; miR, microRNA; NC, negative control; OD, optical density; RA, rheumatoid arthritis.

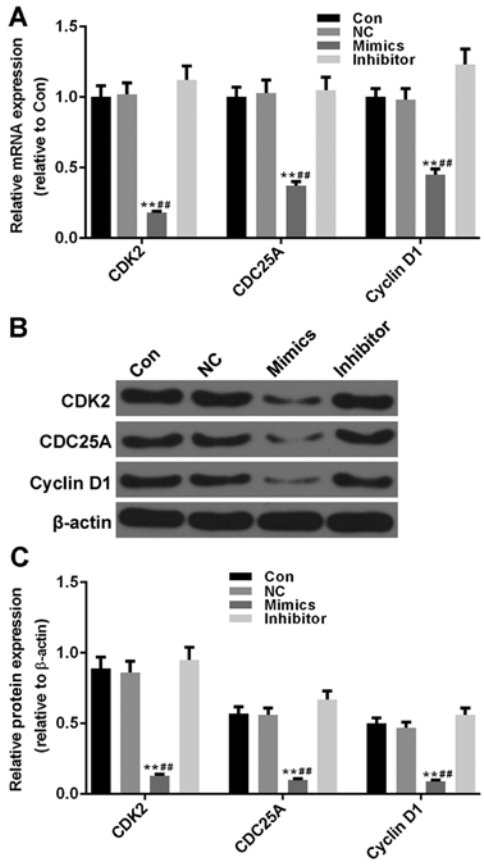

Figure 3. High miR-34-3p expression suppresses the expression levels of cell cycle control genes. (A) mRNA and (B and C) protein expression levels of CDK2, CDC25A and cyclin D1 were measured by reverse transcription-quantitative polymerase chain reaction and western blotting. β-actin was detected as an internal control. Each value represents the mean ± standard deviation (n=3). **P<0.01 vs. Con group; $^{\#\#}$P<0.01 vs. NC group. CDC25A, cell division cycle 25A; CDK2, cyclin-dependent kinase 2; Con, Control group; miR, microRNA; NC, negative control.

miR-34b-3p/5p and miR-34c-3p/5p (15). The onset of OA and RA is associated with oxidative stress and inflammation; therefore, the expression levels of miR-34a-5p were detected in patients with RA and OA and were compared, in order to make the results more conclusive. By comparing the expression levels of miR-34a-3p in RAFLS with those in OAFLS, it was identified that the miR-34a-3p expression was considerably reduced in RAFLS; therefore, it was hypothesized that miR-34a-3p may have an ameliorating effect on RA. To further determine the potential role of miR-34a-3p, overexpression and knockdown of miR-34a-3p were artificially induced, and the proliferation and activation of RAFLS were detected.

Pannus formation is an important characteristic of RA, which is characterized by angiogenic factor-mediated angiogenesis and abnormal hyperplasia of the synovium (23). The pannus, which is composed mostly of FLS, is formed alongside a marked infiltration of lymphocytes and macrophages (24). The increased number of FLS is a key participant in the progression of RA; FLS can attach to articular cartilage and secrete several types of pro-inflammatory cytokines and MMPs to invade the ECM and cartilage, thus inducing severe joint damage and dysfunction (25,26). In the present study, enhanced miR-34a-3p expression significantly inhibited FLS proliferation, which may greatly decrease the production of pro-inflammatory cytokines and MMPs, partly mitigating inflammation and bone destruction in patients with RA. In addition, the CDK family serves a vital role in regulating cell cycle progression; CDK2 can induce the G_1/S transition and promote DNA replication (27). CDC25A and cyclin D1 contribute to activating CDK2, and cyclin D1 can also induce phosphorylation of the retinoblastoma tumor suppressor protein family, activating E2F transcription factors and ultimately driving G_1/S progression (28,29). The results of the present study indicated that increased miR-34a-3p expression

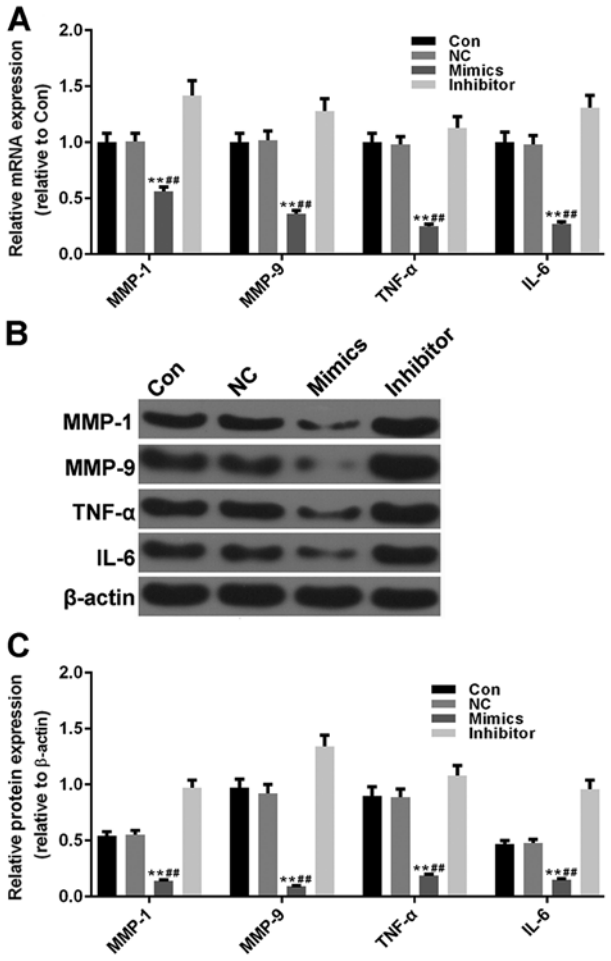

Figure 4. Increased miR-34a-3p expression inhibits MMPs and pro-inflammatory cytokines in rheumatoid arthritis-fibroblast-like synoviocytes. (A) mRNA and (B and C) protein expression levels of MMP-1, MMP-9, TNF-α and IL-6 were measured by reverse transcription-quantitative polymerase chain reaction and western blotting. β-actin was detected as an internal control. Each value represents the mean ± standard deviation (n=3). **P<0.01 vs. Con group; $^{\#\#}$P<0.01 vs. NC group. Con, Control group; IL, interleukin; miR, microRNA; MMP, matrix metalloproteinases; NC, negative control; TNF, tumor necrosis factor.

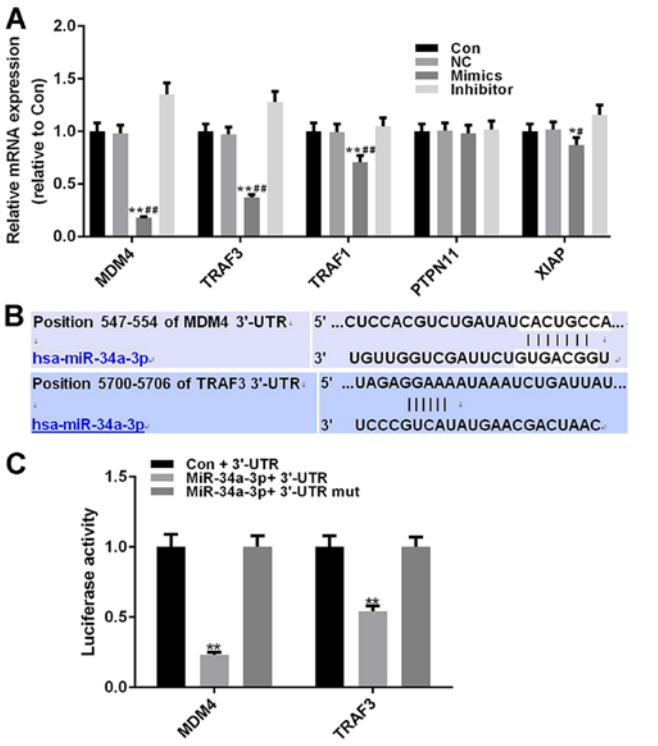

Figure 5. Affinity of miR-34a-3p to MDM4 is stronger compared with TRAF3. (A) mRNA expression levels of five predicted target genes were measured in rheumatoid arthritis-fibroblast-like synoviocytes transfected with miR-34a-3p mimics and inhibitor vectors. β-actin was detected as an internal control. (B) Potential miR-34a-3p binding sites in MDM4 and TRAF3. (C) Luciferase reporter assay further verified whether miR-34a-3p effectively targets MDM4 and TRAF3. Each value represents the mean ± standard deviation (n=3). *P<0.05, **P<0.01 vs. Con + 3'-UTR group; $^{\#}$P<0.05, $^{\#\#}$P<0.01 vs. NC group. 3'-UTR, 3'-untranslated region; Con, Control group; MDM4, murine double minute 4; miR, microRNA; TRAF3 NC, negative control; PTPN11, protein tyrosine phosphatase non-receptor type 11; TNF, receptor-associated factor 3; XIAP, X-linked inhibitor of apoptosis.

may suppress the expression levels of CDK2, CDC25A and cyclin D1, in order to elicit cell cycle arrest of FLS; these results may explain why the number of cells in G_1 phase was much higher in the miR-34a-3p mimics group. MMPs produced by FLS enhance the migration and invasion of FLS, and previous studies have demonstrated that knockdown of SUMO-conjugating enzyme UBC9 or sphingosine kinase 1 notably mitigates the disease progression in RA by blocking the expression of MMPs (30,31). Combined with these studies and the findings of the present study, miR-34a-3p may effectively inhibit cell proliferation, and the migratory and invasive capacities of FLS, and may thus protect articular cartilage from MMPs.

RA is a chronic inflammatory disease, and the functional mechanisms of several inflammatory cytokines have been studied in depth. Previous studies have demonstrated that the expression levels of TNF-α and IL-6 are closely associated with synovitis and joint destruction (32-34). TNF-α stimulation can lead to fibrosis and the inflammatory response of FLS, resulting in production of IL-6, vascular cell adhesion molecule-1 and vascular endothelial growth factor, which participate in the pathophysiology of RA (35,36). In the current study, the expression levels of TNF-α and IL-6 are markedly decreased with increased expression levels of miR-34a-3p, which may suggest that miR-34a-3p expression had the ability to radically decrease inflammation in RA. A previous study demonstrated that coenzyme Q10, an endogenous antioxidant, can effectively downregulate inflammatory cytokines and oxidative stress by inhibiting TNF-α and IL-6 expression levels (37), and tocilizumab is considered a promising agent in RA treatment as it can specifically target IL-6 (38). These data indicate a potential treatment effect of miR-34a-3p on RA.

In the present study, it was suggested that MDM4 may be a potential target gene of miR-34a-3p, according to prediction software (TargetScan and MiRWalk). In addition, the predictions were verified using a luciferase assay, which was helpful in further investigating the molecular mechanism underlying the effects of miR-34a-3p on the pathophysiology of RA. A previous study demonstrated a close association between the expression of MDM4 in FLS and the hyperplasia phenotype of RA synovial tissues (39). Therefore, it was hypothesized that the treatment effect of miR-34a-3p on RA may be dependent on miR-34a-3p effectively silencing MDM4 expression; however, further study is required to confirm this. Niederer *et al* (15) reported that the

mechanism by which miR-34a affects RA may be that miR-34a inhibits apoptosis of RA synovial fibroblasts by upregulating the expression of its direct target XIAP. Another study also identified that miR-34a-deficient mice are resistant to collagen-induced arthritis, and that miR-34a is an epigenetic regulator of dendritic cell function that may contribute to RA, suggesting that RA regression can be aided using a miR-34a inhibitor (40). A previous study also identified that inhibition of miR-34a can improve arthritis in mice by decreasing the percentage of T cells, cytokine expression and bone loss (15). The two possible mature miRNAs of miR-125a, miR-125a-3p and miR-125a-5p, have inverse effects on invasion and migration of lung cancer cells (41). The 3p arm presents more individually regulated targets based on poorly sequence conservation (42). Therefore, the present study hypothesized that miR-34a-3p may exert a protective effect that may different from that of miR-34a-5p in RA. The development of RA is associated with inflammation and immunity, and miR-34a can participate in RA through different pathways. Therefore, further research is required on the mechanism of action of miR-34a in RA. Notably, miR-34a-3p serves a crucial role in the pathogenesis of RA. The present study demonstrated that it may inhibit FLS proliferation and suppress the production of pro-inflammatory cytokines and MMPs, greatly ameliorating articular cartilage destruction. In conclusion, miR-34a-3p may be considered a novel therapeutic target for RA; however, its underlying mechanism requires further research.

Acknowledgements

Not applicable.

Funding

No funding was received.

Availability of data and materials

The datasets used and/or analyzed during the present study are available from the corresponding author on reasonable request.

Authors' contributions

CFH and DW made substantial contributions to the conception and design of the present study. LHZ performed data acquisition, analysis and interpretation. CFH and DW drafted the article and critically revised it for important intellectual content. All authors approved the final version to be published. All authors agreed to be accountable for all aspects of the work in ensuring that questions associated with the accuracy or integrity of the work are appropriately investigated and resolved.

Ethics approval and consent to participate

The present study was approved by the Medical Ethical Review Committee of Jining No. 1 People's Hospital. All procedures performed using human samples were in accordance with the ethical standards of the institutional and/or national research committee and with the 1964 Helsinki declaration and its later amendments or comparable ethical standards. Written informed consent was obtained from all patients.

Patient consent for publication

Not applicable.

Competing interests

The authors declare that they have no competing interests.

References

1. Smolen JS, Aletaha D and McInnes IB: Rheumatoid arthritis. Lancet 388: 2023-2038, 2016.
2. Li ZG, Liu Y, Xu HJ, Chen ZW, Bao CD, Gu JR, Zhao DB, An Y, Hwang LJ, Wang L, *et al*: Efficacy and safety of tofacitinib in chinese patients with rheumatoid arthritis. Chin Med J (Engl) 131: 2683-2692, 2018.
3. Gibofsky A: Overview of epidemiology, pathophysiology, and diagnosis of rheumatoid arthritis. Am J Manag Care 18: S295-S302, 2012.
4. Hawtree S, Muthana M and Wilson AG: The role of histone deacetylases in rheumatoid arthritis fibroblast-like synoviocytes. Biochem Soc Trans 41: 783-788, 2013.
5. Filer A, Ward LSC, Kemble S, Davies CS, Munir H, Rogers R, Raza K, Buckley CD, Nash GB and McGettrick HM: Identification of a transitional fibroblast function in very early rheumatoid arthritis. Ann Rheum Dis 76: 2105-2112, 2017.
6. Hirohata S and Sakakibara J: Angioneogenesis in rheumatoid arthritis. Lancet 354: 423-424, 1999.
7. Danks L, Komatsu N, Guerrini MM, Sawa S, Armaka M, Kollias G, Nakashima T and Takayanagi H: RANKL expressed on synovial fibroblasts is primarily responsible for bone erosions during joint inflammation. Ann Rheum Dis 75: 1187-1195, 2016.
8. Kim HR, Kim KW, Kim BM, Jung HG, Cho ML and Lee SH: Reciprocal activation of CD4+ T cells and synovial fibroblasts by stromal cell-derived factor 1 promotes RANKL expression and osteoclastogenesis in rheumatoid arthritis. Arthritis Rheumatol 66: 538-548, 2014.
9. Jung YK, Kang YM and Han S: Osteoclasts in the inflammatory arthritis: Implications for pathologic osteolysis. Immune Netw 19: e2, 2019.
10. Xiao C and Rajewsky K: MicroRNA control in the immune system: Basic principles. Cell 136: 26-36, 2009.
11. Ruedel A, Dietrich P, Schubert T, Hofmeister S, Hellerbrand C and Bosserhoff AK: Expression and function of microRNA-188-5p in activated rheumatoid arthritis synovial fibroblasts. Int J Clin Exp Pathol 8: 6607-6616, 2015.
12. Tavasolian F, Abdollahi E, Rezaei R, Momtazi-Borojeni AA, Henrotin Y and Sahebkar A: Altered expression of microRNAs in rheumatoid arthritis. J Cell Biochem 119: 478-487, 2018.
13. Ji JD, Kim TH, Lee B, Na KS, Choi SJ, Lee YH and Song GG: Integrated analysis of microRNA and mRNA expression profiles in rheumatoid arthritis synovial monocytes. J Rheum Dis 18: 253-263, 2011.
14. Dang Q, Yang F, Lei H, Liu X, Yan M, Huang H, Fan X and Li Y: Inhibition of microRNA-34a ameliorates murine collagen-induced arthritis. Exp Ther Med 14: 1633-1639, 2017.
15. Niederer F, Trenkmann M, Ospelt C, Karouzakis E, Neidhart M, Stanczyk J, Kolling C, Gay RE, Detmar M, Gay S, *et al*: Down-regulation of microRNA-34a* in rheumatoid arthritis synovial fibroblasts promotes apoptosis resistance. Arthritis Rheum 64: 1771-1779, 2012.
16. Arnett FC, Edworthy SM, Bloch DA, McShane DJ, Fries JF, Cooper NS, Healey LA, Kaplan SR, Liang MH, Luthra HS, *et al*: The American Rheumatism Association 1987 revised criteria for the classification of rheumatoid arthritis. Arthritis Rheum 31: 315-324, 1988.
17. Bailon-Moscoso N, González-Arévalo G, Velásquez-Rojas G, Malagon O, Vidari G, Zentella-Dehesa A, Ratovitski EA and Ostrosky-Wegman P: Phytometabolite dehydroleucodine induces cell cycle arrest, apoptosis, and DNA damage in human astrocytoma cells through p73/p53 regulation. PLoS One 10: e0136527, 2015.
18. Tao K, Yang J, Guo Z, Hu Y, Sheng H, Gao H and Yu H: Prognostic value of miR-221-3p, miR-342-3p and miR-491-5p expression in colon cancer. Am J Transl Res 6: 391-401, 2014.

19. Livak KJ and Schmittgen TD: Analysis of relative gene expression data using real-time quantitative PCR and the 2(-Delta Delta C(T)) method. Methods 25: 402-408, 2001.
20. Bustamante MF, Garcia-Carbonell R, Whisenant KD and Guma M: Fibroblast-like synoviocyte metabolism in the pathogenesis of rheumatoid arthritis. Arthritis Res Ther 19: 110, 2017.
21. Sotillo E, Laver T, Mellert H, Schelter JM, Cleary MA, McMahon S and Thomas-Tikhonenko A: Myc overexpression brings out unexpected antiapoptotic effects of miR-34a. Oncogene 30: 2587-2594, 2011.
22. Mudduluru G, Ceppi P, Kumarswamy R, Scagliotti GV, Papotti M and Allgayer H: Regulation of Axl receptor tyrosine kinase expression by miR-34a and miR-199a/b in solid cancer. Oncogene 30: 2888-2899, 2011.
23. Zhang W, Chen L, Jiang Y and Shen Y: miR-26a-5p regulates synovial fibroblast invasion in patients with rheumatoid arthritis by targeting Smad 1. Med Sci Monit 24: 5178-5184, 2018.
24. Audo R, Deckert V, Daien CI, Che H, Elhmioui J, Lemaire S, Pais de Barros JP, Desrumaux C, Combe B, Hahne M, *et al*: PhosphoLipid transfer protein (PLTP) exerts a direct pro-inflammatory effect on rheumatoid arthritis (RA) fibroblasts-like-synoviocytes (FLS) independently of its lipid transfer activity. PLoS One 13: e0193815, 2018.
25. Ruedel A, Dietrich P, Schubert T, Hofmeister S, Hellerbrand C and Bosserhoff AK: Expression and function of microRNA-188-5p in activated rheumatoid arthritis synovial fibroblasts. Int J Clin Exp Pathol 8: 4953-4962, 2015.
26. Jia W, Wu W, Yang D, Xiao C, Su Z, Huang Z, Li Z, Qin M, Huang M, Liu S, *et al*: Histone demethylase JMJD3 regulates fibroblast-like synoviocyte-mediated proliferation and joint destruction in rheumatoid arthritis. FASEB J 32: 4031-4042, 2018.
27. Bačević K, Lossaint G, Achour TN, Georget V, Fisher D and Dulić V: Cdk2 strengthens the intra-S checkpoint and counteracts cell cycle exit induced by DNA damage. Sci Rep 7: 13429, 2017.
28. Sherr CJ, Beach D and Shapiro GI: Targeting CDK4 and CDK6: From discovery to therapy. Cancer Discov 6: 353-367, 2016.
29. Zhou H, Shen T, Luo Y, Liu L, Chen W, Xu B, Han X, Pang J, Rivera CA and Huang S: The antitumor activity of the fungicide ciclopirox. Int J Cancer 127: 2467-2477, 2010.
30. Li F, Li X, Kou L, Li Y, Meng F and Ma F: SUMO-conjugating enzyme UBC9 promotes proliferation and migration of fibroblast-like synoviocytes in rheumatoid arthritis. Inflammation 37: 1134-1141, 2014.
31. Yuan H, Yang P, Zhou D, Gao W, Qiu Z, Fang F, Ding S and Xiao W: Knockdown of sphingosine kinase 1 inhibits the migration and invasion of human rheumatoid arthritis fibroblast-like synoviocytes by down-regulating the PI3K/AKT activation and MMP-2/9 production in vitro. Mol Biol Rep 41: 5157-5165, 2014.
32. Mo WX, Yin SS, Chen H, Zhou C, Zhou JX, Zhao LD, Fei YY, Yang HX, Guo JB, Mao YJ, *et al*: Chemotaxis of Vδ2 T cells to the joints contributes to the pathogenesis of rheumatoid arthritis. Ann Rheum Dis 76: 2075-2084, 2017.
33. Wei ST, Sun YH, Zong SH and Xiang YB: Serum levels of IL-6 and TNF-α may correlate with activity and severity of rheumatoid arthritis. Med Sci Monit 21: 4030-4038, 2015.
34. Guo Q, Wang Y, Xu D, Nossent J, Pavlos NJ and Xu J: Rheumatoid arthritis: Pathological mechanisms and modern pharmacologic therapies. Bone Res 6: 15, 2018.
35. Nishina N, Kaneko Y, Kameda H, Kuwana M and Takeuchi T: Reduction of plasma IL-6 but not TNF-α by methotrexate in patients with early rheumatoid arthritis: A potential biomarker for radiographic progression. Clin Rheumatol 32: 1661-1666, 2013.
36. Siegfried G, Basak A, Cromlish JA, Benjannet S, Marcinkiewicz J, Chrétien M, Seidah NG and Khatib AM: The secretory proprotein convertases furin, PC5, and PC7 activate VEGF-C to induce tumorigenesis. J Clin Invest 111: 1723-1732, 2003.
37. Abdollahzad H, Aghdashi MA, Asghari Jafarabadi M and Alipour B: Effects of coenzyme Q10 supplementation on inflammatory cytokines (TNF-α, IL-6) and oxidative stress in rheumatoid arthritis patients: A randomized controlled trial. Arch Med Res 46: 527-533, 2015.
38. Kim GW, Lee NR, Pi RH, Lim YS, Lee YM, Lee JM, Jeong HS and Chung SH: IL-6 inhibitors for treatment of rheumatoid arthritis: Past, present, and future. Arch Pharm Res 38: 575-584, 2015.
39. Xu N, Wang Y, Li D, Chen G, Sun R, Zhu R, Sun S, Liu H, Yang G and Dong T: MDM4 overexpression contributes to synoviocyte proliferation in patients with rheumatoid arthritis. Biochem Biophys Res Commun 401: 417-421, 2010.
40. Kurowska-Stolarska M, Alivernini S, Melchor EG, Elmesmari A, Tolusso B, Tange C, Petricca L, Gilchrist DS, Di Sante G, Keijzer C, *et al*: MicroRNA-34a dependent regulation of AXL controls the activation of dendritic cells in inflammatory arthritis. Nat Commun 8: 15877, 2017.
41. Jiang L, Huang Q, Zhang S, Zhang Q, Chang J, Qiu X and Wang E: Hsa-miR-125a-3p and hsa-miR-125a-5p are downregulated in non-small cell lung cancer and have inverse effects on invasion and migration of lung cancer cells. BMC Cancer 10: 318, 2010.
42. Córdova-Rivas S, Fraire-Soto I, Mercado-Casas Torres A, Servín-González LS, Granados-López AJ, López-Hernández Y, Reyes-Estrada CA, Gutiérrez-Hernández R, Castañeda-Delgado JE, Ramírez-Hernández L, *et al*: 5p and 3p strands of miR-34 family members have differential effects in cell proliferation, migration, and invasion in cervical cancer cells. Int J Mol Sci 20, 2019.

This work is licensed under a Creative Commons Attribution-NonCommercial-NoDerivatives 4.0 International (CC BY-NC-ND 4.0) License.